UDK 629.3.027.521:343.982.34
Original scientific article/Izvirni znanstveni članek

ISSN 1580-2949
Mater. Tehnol.

THE EFFECT OF WAX EMULSION ON THE PERFORMANCE OF CHROMIUM-FREE ANTI-FINGERPRINT PASSIVATION FILM

VPLIV VOŠČENE EMULZIJE NA UČINKOVITOST PASIVACIJSKEGA FILMA BREZ KROMA PROTI PRSTNIM ODTISOM

Zhenqian Zhang[1], Deyi Zhang[1], Yulong Li[1], Jinpeng Liang[2], Jian Li[2], Xiaohua Liu[2], Yi Wang[1]*

[1]School of Petrochemical Technology, Lanzhou University of Technology, Lanzhou 730050, China
[2] Gansu Jiu Gang Group Hongxing Iron and Steel Co., Ltd., Gansu 73500, China

Prejem rokopisa – received: 2025-10-10; sprejem za objavo – accepted for publication: 2026-02-02

doi:10.17222/mit.2025.1588

Limited research exists on the passivation film of anionic waterborne polyurethane resin, particularly regarding strategies to enhance its performance. This study investigates the influence of the wax emulsion's particle size and concentration on the structure, interfacial behavior, corrosion resistance, friction resistance, and adhesion properties of the passivation film. Findings reveal that using a 450-nm wax-emulsion particle size and a 2 % addition yield a composite passivation film characterized by a high surface gloss, low roughness, and exceptional friction resistance. Notably, while maintaining adhesion, the corrosion resistance is improved, thereby enhancing the overall performance of the passivation film. This research sheds light on the effects of wax emulsion on the performance of passivation films, providing valuable insights for optimizing anionic waterborne polyurethane-resin passivation films in future studies.

Keywords: chromium-free fingerprint-resistant passivation film, hot-dip aluminum-zinc plating, Anionic waterborne polyurethane resin, wax emulsion

Dosedanjih raziskav o pasivacijskih prevlekah na osnovi anionske poliuretanske smole na vodni osnovi je relativno malo, zlasti glede strategij za izboljšanje njene učinkovitosti. V tem članku avtorji zato predstavljajo študijo, ki je preučevala vpliv velikosti in koncentracije delcev voščene emulzije na strukturo, medfazno obnašanje, korozijsko odpornost, odpornost proti trenju in adhezijske lastnosti pasivacijskih filmov. Ugotovitve študije so pokazale, da uporaba delcev voščene emulzije velikosti 450 nm in 2-odstotnega dodatka dajejo kompozitni pasivacijski flim, za katerega so značilni visok površinski sijaj, majhna hrapavost in izjemna odpornost proti trenju. Poleg tega avtorji povdarjajo, da se ob ohranjanju adhezije znatno izboljša korozijska odpornost, s čimer se je izboljšala tudi njegova splošna učinkovitost. S to raziskavo so avtorji za bodoče raziskave na tem področju pojasnili učinke voščene emulzije na učinkovitost pasivacijskih filmov in predstavili dragocene napotke za optimizacijo anionskih pasivacijskih filmov iz poliuretanske smole na vodni osnovi.

Ključne besede: pasivizacijska prevleka brez kroma odporna na prstne odtise, vroče potaplanje, aluminijasto-cinkova prevleka, anionska poliuretanska smola na vodni osnovi, voščena emulzija

1 INTRODUCTION

The stringent enforcement of global environmental regulations and the increasing adoption of sustainable development principles have led to restrictions or a discontinuation of the chromate-passivation process in traditional metal surface treatments due to its high toxicity and environmental impact.[1–4] Consequently, the development of effective, eco-friendly, chromium-free passivation technologies has emerged as a crucial research focus in metal protection.[5–9] Water-borne polyurethane resins are widely used in various applications, including biomedical uses, glass-fiber sizing, adhesives, automotive finishes, passivation films, and other coatings, due to their exceptional adhesion, abrasion resistance and versatility.[10–13] Specifically, anionic waterborne polyurethane resins can form a stable bond with metal substrates via electrostatic interactions mediated by carboxylate or sulfonate groups in their molecular structure. These resins also confer the coating with excellent hydrolysis resistance and mechanical strength, making them ideal for developing fingerprint-resistant passivation films.[14–17] Nonetheless, stand-alone water-borne polyurethane coatings encounter challenges such as fingerprint residues, inadequate anti-fouling properties, and limited long-term corrosion resistance, necessitating urgent functional modifications to enhance performance.

In recent years, advances have been made in enhancing the overall efficacy of chromium-free passivation films through the incorporation of nanomaterials, organosilanes, and polymer composite coatings, among other innovations.[18–22] Wax emulsions have emerged as a notable focus in this area owing to their distinctive physical and chemical attributes. Serving as eco-friendly functional additives, wax emulsions exhibit the potential for chromium-free passivation systems.[23] Upon curing,

*Corresponding author's e-mail:
wangyi@lut.edu.cn (Yi Wang)

they facilitate the formation of a low-surface-energy, hydrophobic film layer, effectively impeding the adhesion and diffusion of fingerprint oils. Simultaneously, they retard the ingress of corrosive agents through a physical barrier mechanism.[24,25] A significant synergistic interaction is observed between an anionic waterborne polyurethane resin and a wax emulsion. The anionic groups within the polyurethane molecular structure stabilize the wax emulsion dispersion system via electrostatic interactions, thereby preventing the aggregation of nanowax particles.[26]

Furthermore, the incorporation of a wax emulsion helps fill the minute pores in the cross-linked polyurethane network, thereby enhancing the compactness of the passivation film. By judiciously selecting wax varieties with favorable compatibility with polyurethane, such as oxidized polyethylene wax and Fischer-Tropsch wax, and by controlling the particle-size distribution of the emulsion during curing, the surface morphology and dynamic hydrophobic properties of the coating can be further fine-tuned. This optimization strategy enables the concurrent enhancement of fingerprint resistance and corrosion resistance.

Research on wax-emulsion-modified anionic waterborne polyurethane passivation films has shown initial progress, yet challenges remain for industrial implementation. Balancing the hydrophobicity and coating adhesion of a wax emulsion is challenging, as excessive amounts can weaken interfacial bonding. The molecular structure of anionic polyurethane, including the ratios of hard and soft segments and the hydrophilic group content, influences the dispersion stability of wax emulsions and the film uniformity. However, there is a lack of systematic research on the structure-activity relationship. This study addresses these issues by examining the composite system comprising an anionic waterborne polyurethane resin and a wax emulsion. It systematically investigates the functional role of the wax emulsion in chromium-free fingerprint-resistant passivation films, explores its synergistic mechanisms with the passivation system, and assesses its effects on corrosion resistance, fingerprint resistance, and the coating's mechanical properties. The aim is to offer a theoretical foundation and technical backing for developing environmentally friendly, high-performance metal protective coatings.

2 EXPERIMENTAL PART

2.1 Experimental materials

The experimental substrates used were DC53D+AZ hot-dip aluminum-zinc-coated carbon steel sheets, manufactured by the Carbon Steel Sheet Plant of Hongxing Iron and Steel Co., Ltd., Jiuquan Iron and Steel (Group) Co., Ltd., with a thickness of 1 mm. These substrates were laser-cut into 100 mm × 70 mm × 1 mm specimens and subsequently deburred. Following activation through acetone immersion, rinsing with distilled water, and drying with absorbent cotton, the specimens were prepared for further analysis. The waterborne polyurethane resin (PU-4001) was sourced from Hefei Puqing New Material Technology Co., Ltd. The surfactant (FS-660) was obtained from Tianjin Hepufeile New Material Co., Ltd. Waterborne wax emulsions (GA-1806, GA-2000, GT-3360) were procured from Foshan Wengkai'er Trading Co., Ltd., with all other reagents meeting analytical grade standards.

2.2 Experimental methods

The waterborne polyurethane resin was thinned in a 1:1 ratio and combined with a surfactant and wax emulsions. Following 10 min of ultrasonic treatment at room temperature, a composite passivation solution was produced. Three wax emulsions with different particle sizes were chosen. Subsequently, the passivation solution was evenly applied onto the substrate surface using a wire rod coater. The thickness of the dry passivation layer was adjusted to fall within the range of 0.8–1.2 g/m^2, corresponding to a physical film thickness of approximately 1 μm. Lastly, the coated substrate was dried at 190 °C for 2 min to prepare it for utilization.

To investigate the composition and microstructure of the wax emulsion and passivation film, the wax emulsion was dried in a freeze dryer (DYYB-10, Shanghai Deyang Yibang Instrument Co., Ltd.), ground into powder, and analyzed by infrared spectroscopy using an IS5 spectrometer (Thermo Fisher Scientific) to identify its components. The passivation film was analyzed by X-ray photoelectron spectroscopy using an ESCALAB 250Xi spectrometer (Thermo Fisher Scientific, USA) equipped with an Al-Kα X-ray source (1486.68 eV). The surface morphology of the composite passivation film was analyzed using a field emission scanning electron microscope (Sigma 300, Zeiss, Germany).

To assess the impact of wax emulsion on the interfacial behavior of the passivation film, we employed a contact angle tester (SZ-CAMC33, Shanghai Xuanhuai Instrument Co., Ltd.) to quantify the contact angle of the passivated metal sample. Surface gloss was determined using a gloss meter (LS195, Shenzhen Linshang Technology Co., Ltd.), while surface roughness was analyzed with a laser confocal microscope (OLS500, Olympus Corporation, Japan). The combined analysis of contact angle, gloss, and surface roughness provided a comprehensive evaluation of the effect of wax emulsion on the passivation film's surface characteristics.

To assess the impact of wax emulsions on the corrosion resistance of passivation films, we conducted a 72-hour neutral salt-spray test on samples in a salt-spray chamber (LYW-015, Shanghai Yiheng Scientific Instrument Co., Ltd.) following the national standard "Corrosion tests in artificial atmospheres – Salt spray tests" (GB/T 10125-2012). This evaluation aimed to compare the corrosion resistance of samples coated with wax emulsions varying in particle sizes and concentrations.

The salt-spray test maintained a temperature of 35 ± 2 °C, a humidity of 95 %, a salt spray settling rate of 1–2 mL/(h·cm^2), and a nozzle pressure of 48.3–148.2 kPa. An electrochemical workstation (Ivium Vertex, Tianjin Deshang Technology Co., Ltd.) was employed to analyze the electrochemical properties of the passivation films. The setup included a platinum auxiliary electrode, a saturated calomel reference electrode, and a hot-dip aluminized zinc carbon-steel sheet sample with a passivation film as the working electrode. The electrolyte used was 3.5 *w*/% NaCl, and the test temperature remained constant at 25 °C, with a sample surface area of 1 cm^2. For the electrochemical impedance test, the initial potential corresponded to the passivation film's stable open-circuit potential. The test frequency range spanned from 10^{-1} Hz to 10^5 Hz, with a sinusoidal excitation signal of 10 mA, and a scanning rate of 1 mV/s for the polarization curve.

To assess the impact of the wax emulsion on the adhesion of the passivation film, a paint sprayer (F-75G, China Delixi Electric Co., Ltd.) was utilized to uniformly apply Hardtop WF water-borne polyurethane topcoat (6DX) onto the passivation film's surface. Subsequently, the coating resistance of the passivation film was evaluated in accordance with the national standard GB/T 9286-2021, "Paints and varnishes – Cross-cut test," after the paint had air-dried. A clean cotton ball was then moistened with a small quantity of Vaseline and evenly spread over half of the sample surface. After 30 min, the Vaseline was removed using a clean cotton ball. The fingerprint resistance of the passivation film was assessed following national standards GB/T 11186.2-1989 "Methods for measurement of film color – Part 2: Color measurement" and GB/T 11186.3-1989 "Methods for measurement of film color – Part 3: Calculation of color difference." The impact of the wax emulsion on the adhesion of the passivation film was comprehensively evaluated based on its coating resistance and fingerprint resistance.

To assess the impact of the wax emulsion on the friction resistance of the passivation film, we employed a high-speed ring-block wear tester (MRH-3A, Jinan Yihua Tribology Testing Technology Co., Ltd.) to perform friction resistance testing on passivation film-coated samples. Test conditions included a 30-N load, a rotation speed of 30 min^{-1}, and a temperature of 25 °C. The influence of the wax emulsion on the friction resistance of the passivation film was determined by analyzing variations in the friction coefficient.

3 RESULTS AND DISCUSSION

3.1 Structural characterization of passivation film

This investigation examines the impact of three wax emulsions, namely GA-1806, GA-2000, and GT-3360, each characterized by distinct particle sizes, on diverse properties of the passivation film. **Figure 1a** illustrates the schematic representation of the passivation film after the incorporation of the wax emulsion. The spherical morphology of the paraffin particles confers favorable dispersibility and mechanical properties to the emulsion, thereby laying the groundwork for enhancing the performance of the passivation film. Varied particle sizes of paraffin particles engender channels with uneven spacing on both the surface and within the passivation film. Owing to paraffin's hydrophobic nature and poor compatibility with polyurethane, these particles migrate towards the film's surface throughout the film-forming process, resulting in a distinctive pattern characterized by enrichment on the surface layer and sparsity inside. The particle size of the wax emulsion profoundly influences its dispersion within the polyurethane resin. Optimal particle size selection is crucial for achieving a balance between dispersion uniformity and stability, thereby influencing factors such as corrosion resistance, friction resistance, and the adhesion of the passivation film.

Three distinct wax emulsions, namely GA-1806, GA-2000, and GT-3360, were diluted 100-fold with deionized water, and their particle sizes were assessed using a nano laser particle-size analyzer. The findings are depicted in **Figure 1c-1e**. The data reveal that the mean particle sizes of GA-1806, GA-2000, and GT-3360 are 608.16 nm, 445.31 nm, and 355.3 nm, respectively, and exhibit typical distributions. The spans for GA-1806, GA-2000, and GT-3360 are approximately 1.62, 1.14, and 0.67, respectively. Notably, there is a gradual reduction in particle-size dispersion across the samples, leading to improved particle-size uniformity.

Figure 1b displays the infrared spectra of the standard wax emulsion GA-2000 and pure paraffin. Both spectra exhibit prominent absorption peaks at 2920 cm^{-1} and 2850 cm^{-1}, indicative of a saturated alkane framework. Additionally, absorption peaks at approximately 1460 cm^{-1} and 1370 cm^{-1} confirm the presence of saturated alkane structures in both samples. The characteristic absorption peak at 720 cm^{-1}, typical of long-chain alkanes, is consistent with the paraffin composition in both spectra. Notably, the infrared spectrum of GA-2000 reveals a distinct stretching vibration peak at 1115 cm^{-1} corresponding to C-O-C, suggesting the incorporation of a non-ionic emulsifier during its preparation.[27] This emulsifier facilitates the interaction between the alkyl portion of paraffin and the oxyethylene ether bond, leading to the formation of an amphiphilic cooperative structure. In this structure, the hydrophobic end anchors the paraffin while the hydrophilic end interfaces with the aqueous phase. This transformation renders the paraffin hydrophilic and stably dispersible, enhancing its stability and compatibility without compromising its original properties.

The surfaces of dispersed particles of anionic waterborne polyurethane resin typically bear anionic groups, such as carboxyl and sulfonic acid groups. In contrast, wax emulsions utilize non-ionic emulsifiers, re-

sulting in neutral or weakly negative surface charges on the paraffin particles. Consequently, the electrostatic repulsion between the paraffin particles and the anionic polyurethane is minimal, facilitating enhanced particle adsorption through other forces. Paraffin, a low-polarity long-chain alkane, exhibits a stark polarity contrast with the polar group-containing molecular chains of anionic polyurethane. Nevertheless, in the aqueous dispersion of polyurethane, the hydrophilic groups on particle surfaces can attract polyoxyethylene chains from the non-ionic emulsifier in the wax emulsion via hydrogen bonding or dipole interactions. The polyoxyethylene chains of the non-ionic emulsifier can establish hydrogen bonds with the polar groups of polyurethane, with the hydrophobic end anchoring the wax particles, thereby reducing the interfacial energy, enhancing the compatibility, and stabilizing the mixed system. Additionally, dispersion forces operate between the molecular segments of the wax and polyurethane particles, particularly when the paraffin carbon chain's length aligns with the polyurethane soft segment, resulting in closer intermolecular contact and stronger interactions.

The microstructure of the passivation film was examined using a field-emission scanning electron microscope. **Figures 2a** and **2b** present low-magnification SEM images of samples coated with a resin-based passivation film and a wax-emulsion composite passivation film, respectively. Both surfaces exhibit a uniform reticular structure. **Figures 2c** and **2d** show high-magnification SEM images. As shown in **Figure 2c**, the resin passivation film develops numerous cracks after high-temperature drying, potentially providing pathways for corrosive media to penetrate and attack the underlying carbon steel substrate.

In contrast, when wax emulsion is incorporated, paraffin particles effectively fill these cracks, resulting in a significantly denser film structure, as illustrated in **Figure 2d**. The elimination of cracks enhances the barrier properties of the passivation film against the corrosive species, thereby improving its corrosion resistance. Furthermore, the presence of paraffin particles on the surface enhances the wear resistance and imparts a degree of self-healing to the passivation film.

To further analyze the chemical composition and molecular structure of the passivation film, full-spectrum X-ray photoelectron spectroscopy (XPS) was performed on the passivation film treated with the standard wax emulsion GA-2000. The results, depicted in **Figure 3a** and summarized in **Table 1**, reveal that the passivation film predominantly comprises carbon (C), oxygen (O), nitrogen (N), and silicon (Si), constituting atomic percentages of 58.46 %, 37.46 %, 2.64 %, and 1.44 %, respectively. The carbon component primarily originates from the carbon chains in the polyurethane resin and paraffin wax. The oxygen is derived from the non-ionic emulsifier within the wax emulsion and anionic groups like carboxyl groups in the polyurethane resin. Nitrogen and silicon are sourced mainly from the isocyanate in the polyurethane resin and the organic wax silicon in the wax emulsion.

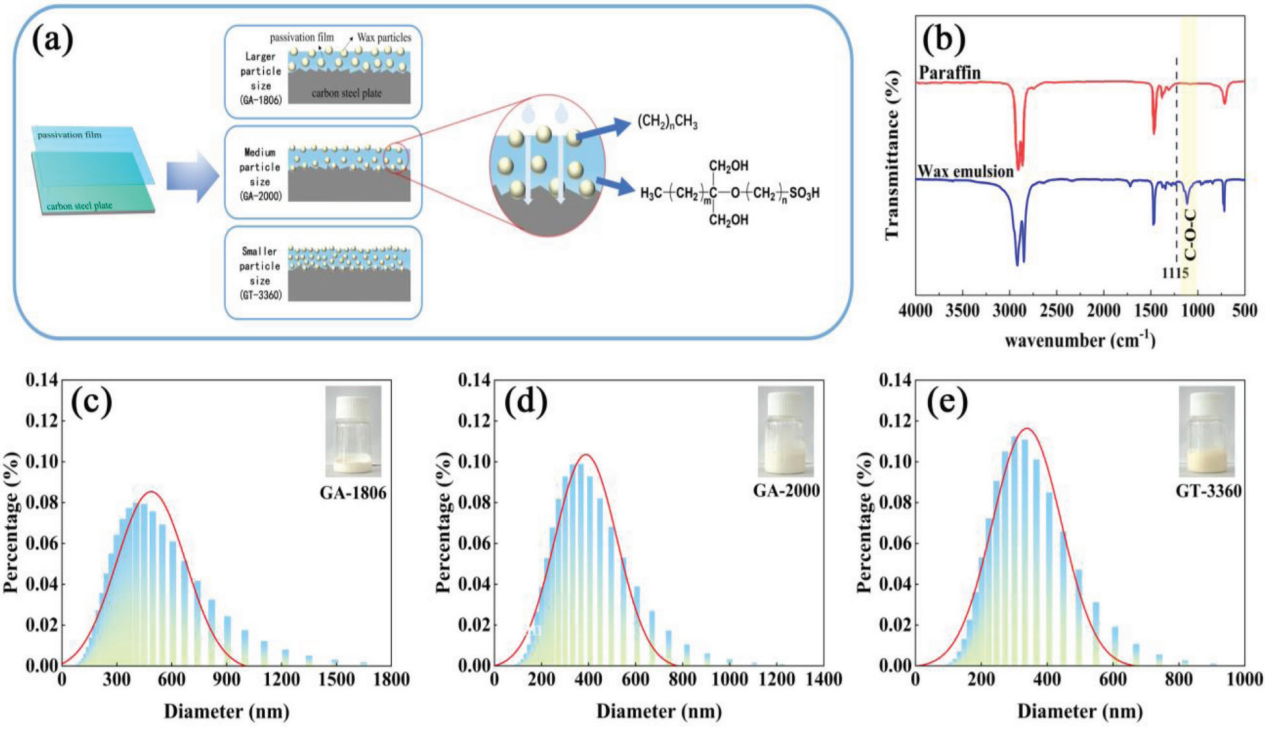

Figure 1: Structural characterization diagrams of wax emulsion: a) Schematic representation of the passivation film structure; b) Fourier-transform infrared spectroscopy (FT-IR) spectra comparing paraffin with the wax emulsion; and c)-e) Particle size distribution profiles for GA-1806, GA-2000, and GT-3360, respectively.

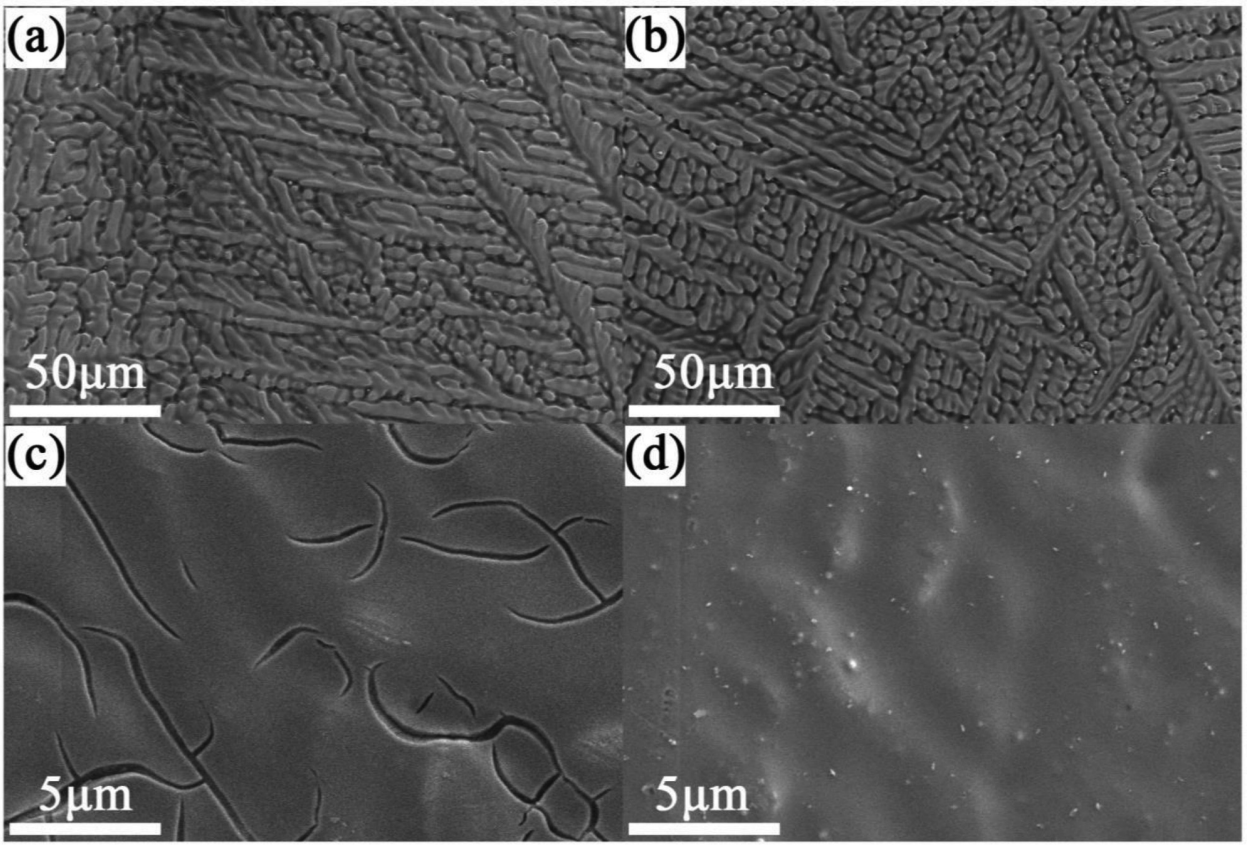

Figure 2: SEM results of passivation films: a) and c) are samples with resin-coated passivation films; b) and d) are samples with wax emulsion composite passivation films

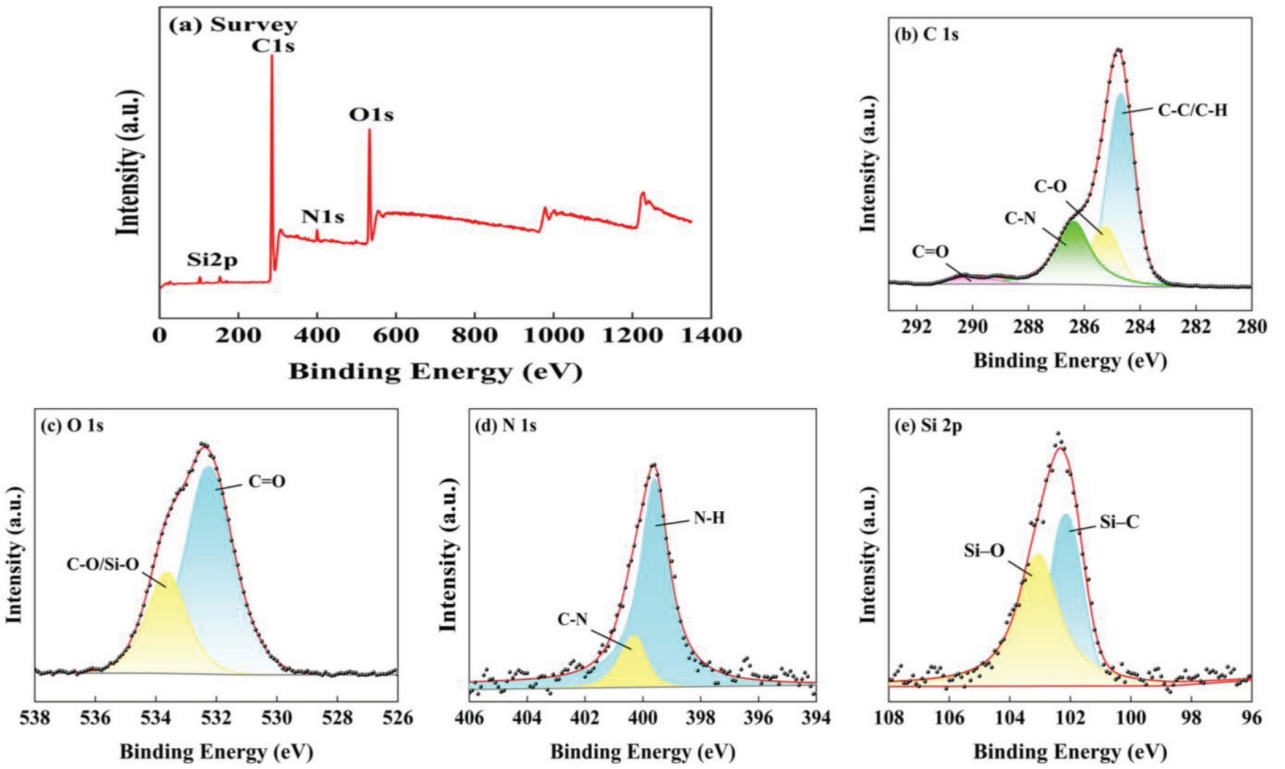

Figure 3: XPS spectra of the passivation film: a) Full XPS spectrum; b) High-resolution C1s orbital XPS spectrum; c) High-resolution O1s orbital XPS spectrum; d) High-resolution N1s orbital spectrum; e) High-resolution Si2p orbital XPS spectrum.

Table 1: Major elements detected in the passivation film via X-ray photoelectron spectroscopy

	C	O	N	Si
Binding energy (eV)	285.13	532.87	399.97	102.39
Atomic conc. (%)	58.46	37.46	2.64	1.44
Mass conc. (%)	50.92	43.46	2.68	2.94

To analyze the chemical states of various elements in the passivation film, high-resolution scanning was conducted to examine the chemical states of multiple elements (C, O, N, and Si) within the passivation film. The fitting process used the Gaussian/Lorentzian least-squares Shirley background-subtraction method. The outcomes are depicted in **Figures 3b-3e**.

Figure 3b depicts the high-resolution X-ray photoelectron spectroscopy (XPS) analysis of the C1s orbital within the passivation film, revealing four discernible peaks. Specifically, the peak at 284.6 eV corresponds to the C-C/C-H bond, 286.2 eV to the C-O bond, 285.3 eV to the C-N bond, and 289.6 eV to the C=O bond.[28] These findings suggest that carbon within the passivation film predominantly exists in the forms of C-C/C-H, C-O, C-N, and C=O. The presence of C-C and C-H bonds is attributed to the paraffin structure of the wax emulsion and to the polyurethane resin's carbon-chain structure. At the same time, C-O and C=O are primarily derived from the anionic groups present in the waterborne polyurethane resin.

Figure 3c displays the high-resolution X-ray photoelectron spectroscopy (XPS) spectrum of the O1s orbital within the passivation film. The peak at 533.7 eV corresponds to the C-O/Si-O bond, while the peak at 532.2 eV corresponds to the C=O bond.[29] Oxygen within the composite passivation film is present in the forms of C-O/Si-O and C=O, primarily originating from the non-ionic emulsifier in the wax emulsion and the anionic groups in the waterborne polyurethane resin.

Figure 3d displays the high-resolution X-ray photoelectron spectroscopy (XPS) spectrum of the N1s orbital within the passivation film. The peaks at 399.6 eV and 400.3 eV are attributed to C-N and N-H bonds, respectively.[30] This suggests that nitrogen in the composite passivation film is present in the C-N and N-H forms, primarily originating from the isocyanate and chain-extender components in the waterborne polyurethane.

Figure 3e displays the high-resolution X-ray photoelectron spectroscopy (XPS) spectrum of the Si2p orbital within the passivation film. This spectrum reveals two distinct peaks at 102.2 eV and 103.1 eV, attributed to the Si-C and Si-O bonds, respectively.[31] These findings suggest that silicon within the composite passivation film predominantly exists in the Si-C and Si-O forms, originating primarily from the organic wax silicon present in the wax emulsion.

3.2 Influence of wax emulsion on the interfacial behavior of passivation film

The gloss and surface roughness of metal samples coated with a composite passivation film were analyzed, as shown in Figures 4a and 4b. Incorporating wax emulsion can effectively fill surface defects in the passivation film, such as gaps, cracks, and pits. However, the wax-emulsion particles do not chemically react with the galvanized layer, but are instead dispersed on the film's surface and within it.[32] The size of the wax-emulsion particles influences the gloss and surface roughness of the passivation film. Increasing the amount of wax emulsion leads to a higher surface roughness of the composite passivation film, as illustrated in **Figure 4a**. Specifically, at a 1 % wax emulsion addition rate, the composite passivation film with GT-3360 wax emulsion has the highest surface roughness.

In contrast, films with GA-2000 and GA-1806 wax emulsions exhibit relatively lower and similar roughness levels. The smaller paraffin particle size in GT-3360 wax emulsion results in a higher number of semi-embedded particles on the polyurethane resin film's surface, thereby increasing the roughness. In contrast, the larger paraffin particles in GA-2000 and GA-1806 wax emulsions yield a moderate number of embedded particles

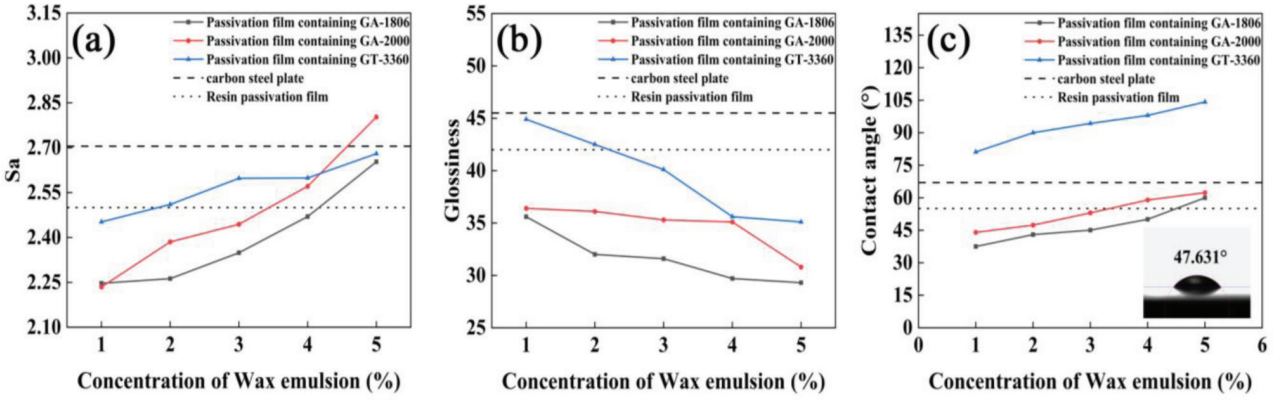

Figure 4: Effects of wax emulsions on the surface condition of the passivation film: a) depicts the changes in surface roughness based on the type and quantity of wax emulsions added; b) shows the alterations in gloss levels corresponding to different types and quantities of wax emulsions; and c) displays the variations in contact angle as influenced by the type and quantity of wax emulsions.

within the polyurethane resin film, exerting less influence on surface morphology and resulting in a lower surface roughness. As the addition rate increases, more paraffin particles become semi-embedded on the film's surface, consequently elevating the surface roughness. Moreover, the surface roughnesses of the samples coated with the composite passivation film are notably lower than that of bare plates lacking the passivation film. This reduction in roughness is attributed to the passivation film filling surface pits on the bare plates, thereby enhancing the surface smoothness. Gloss reflects the intensity of light's diffuse reflection on an object's surface. Higher gloss indicates a stronger diffuse reflection, resembling a mirror effect. Conversely, lower gloss signifies weaker diffuse reflection. Surface gloss is influenced by the physical and chemical properties of the passivation film and by the surface roughness. When surface roughness exceeds the incident light's wavelength, diffuse reflection intensifies alongside the specular reflection, reducing gloss. The relationship between surface gloss and surface roughness is inversely proportional, as observed in **Figure 4b**, underscoring the adverse impact of the surface roughness on gloss. Coated samples exhibit significantly lower surface gloss than bare plates due to the stronger surface diffuse reflection of light on metals compared to that on the organic passivation film layer. Consequently, applying the composite passivation film weakens the surface diffuse reflection, resulting in decreased gloss.

The impact of a composite passivation film on the contact angle of the metal samples was examined, as depicted in **Figure 4c**. The introduction of a wax emulsion was found to increase the contact angle of the passivated surface, reduce surface tension, and shorten the duration of corrosive droplets on the film surface.[33] Contact angles across all samples increased proportionally with increasing wax-emulsion concentration, attributed to the pronounced hydrophobicity of the alkyl carbon chains in the paraffin particles. Notably, the passivation film treated with GT-3360 wax emulsion exhibited the highest surface contact angle, while that treated with GA-2000 wax emulsion displayed the lowest, with GA-1806 wax emulsion falling in between. The contact angle exhibited an inverse relationship with both the quantity and size of wax emulsion particles. It was influenced by the presence of semi-embedded particles on the surface of the polyurethane resin film. Specifically, at identical concentrations, the passivation film treated with the GT-3360 wax emulsion (with the smallest particle size) exhibited the highest number of paraffin particles, resulting in enhanced hydrophobicity and a higher contact angle. Moreover, increasing the amount of wax emulsion led to a greater number of semi-embedded paraffin particles on the polyurethane resin surface, further elevating the contact angle. The contact angle serves as a direct indicator of the passivation film's surface energy. Excessively high contact angles may intensify the surface hydrophobicity, potentially leading to coating detachment from the metal substrate due to inadequate adhesion and thereby compromising corrosion resistance. Conversely, excessively low contact angles may heighten the risk of corrosion medium infiltration owing to excessive surface hydrophilicity.

3.3 Influence of wax emulsion on the corrosion resistance of passivation film

A 72-hour neutral salt-spray test was conducted on samples coated with polyurethane passivation films containing wax emulsions of varying particle sizes, as depicted in **Figure 5**. The incorporation of a wax emulsion seals micronano defects within the coating, imparting hydrophobicity that reduces the interaction between corrosive droplets and the coating surface, thereby enhancing its corrosion resistance.[34–36] A comparison of **Figures 5a-5f** reveals a notable improvement in corrosion resistance in samples coated with a composite passivation film containing 2 % GA-2000 wax emulsion, as opposed to those coated with polyurethane passivation film lacking wax emulsion. Specifically, the corrosion area decreased significantly from 19.26 % to 1.45 %. Metallographic images show that after the post-salt-spray test, the sample coated with a wax-free polyurethane passivation film exhibited extensive surface corrosion, including bottomless pits, covering 42.31 % of the observed area (**Figure 5b**).

In contrast, the sample coated with the composite passivation film displayed shallow pitting corrosion, covering only 7.81 % of the observed area (**Figure 5e**). Laser confocal microscopy images of the samples show substantial corrosion product accumulation on the wax-free polyurethane-coated sample post-test, with a stack height of approximately 3.878 μm (**Figure 5c**). Conversely, the composite passivation film-coated sample exhibited minimal pitting corrosion and significantly reduced corrosion depth (**Figure 5f**), indicating improved corrosion resistance. **Figure 5** demonstrates the impact of the wax-emulsion particle size and quantity on the sample's corrosion resistance. Notably, passivation films containing the GT-3360 wax emulsion exhibited the highest corrosion resistance, owing to the smaller paraffin particle size in GT-3360, which effectively impedes the penetration of corrosive liquids into the film. The corrosion resistance initially decreases and then increases with increasing wax emulsion quantity. Samples coated with a composite passivation film containing 2 % GA-2000 wax emulsion demonstrated optimal corrosion resistance, closely approaching that of films with the same amount of GT-3360 wax emulsion. Films containing GT-3360 and GA-1806 wax emulsions displayed peak corrosion resistance at a 3 % addition rate. Excessive addition of wax emulsion may lead to uneven dispersion of paraffin particles within the polyurethane

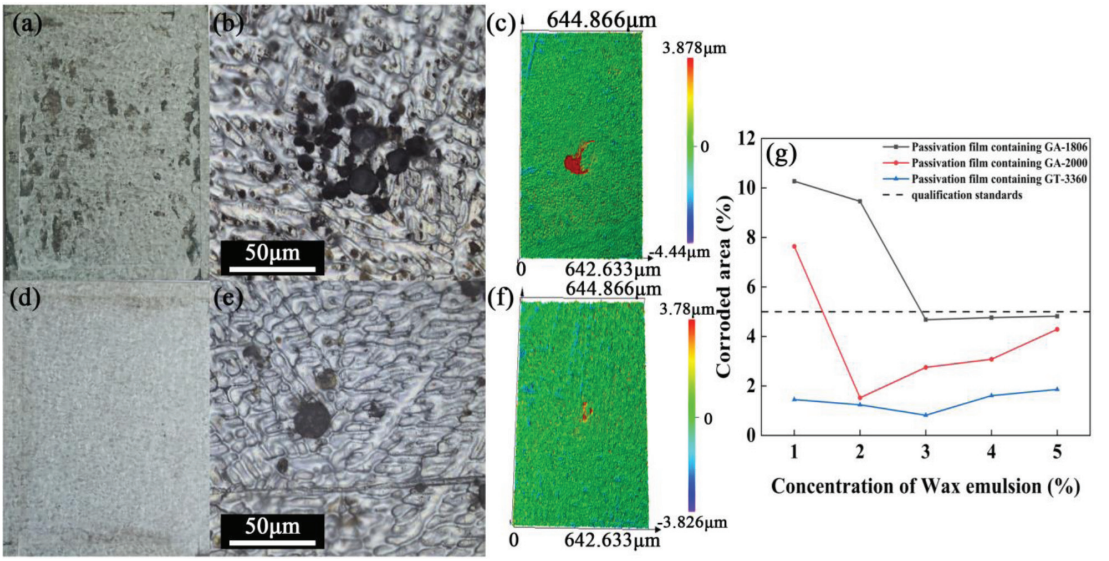

Figure 5: Results of salt spray test: a), b), and c) are the optical photos, metallographic photos, and 3D surface morphology diagrams of the coated resin passivation film samples after salt spray; d), e), and f) are the optical photos, metallographic photos, and 3D surface morphology diagrams of the coated samples with added GA-2000 composite passivation film after salt spray; g) is the salt-spray test result diagram.

resin, resulting in particle aggregation and, subsequently, affecting sample corrosion resistance.

Impedance and Tafel curve analyses were performed on both the bare carbon steel plate and samples coated with composite passivation films containing a consistent 2 % wax emulsion. The test findings are presented in **Figure 6**. The arc diameter in the impedance spectrum corresponds to the charge transfer resistance (R_{ct}), with a larger diameter indicating higher corrosion resistance of the respective sample. Notably, a single arc is observed in the impedance spectrum of the specimen coated with the composite passivation film, suggesting a uniform and defect-free passivation film. The arc radius of the passivation film-coated specimen surpasses that of the bare carbon steel plate, with the largest arc radius observed for the passivation film incorporating GT-3360 wax emulsion, signifying a substantial enhancement in corrosion resistance upon wax-emulsion addition. The passivation film containing the GT-3360 wax emulsion exhibits the best corrosion resistance (**Figure 6a**).In the Tafel curve analysis, a positive shift in corrosion potential is observed for specimens coated with the passivation film compared to bare carbon steel. The self-corrosion current density of the passivation film incorporating GT-3360 wax emulsion is the lowest, with self-corrosion potential and current density values of –0.946 V and 3.17×10^{-6} A·cm^{-2}, respectively. Notably, at a 2 % wax emulsion content, GT-3360 demonstrates commendable corrosion resistance and a reduced corrosion rate, consis-

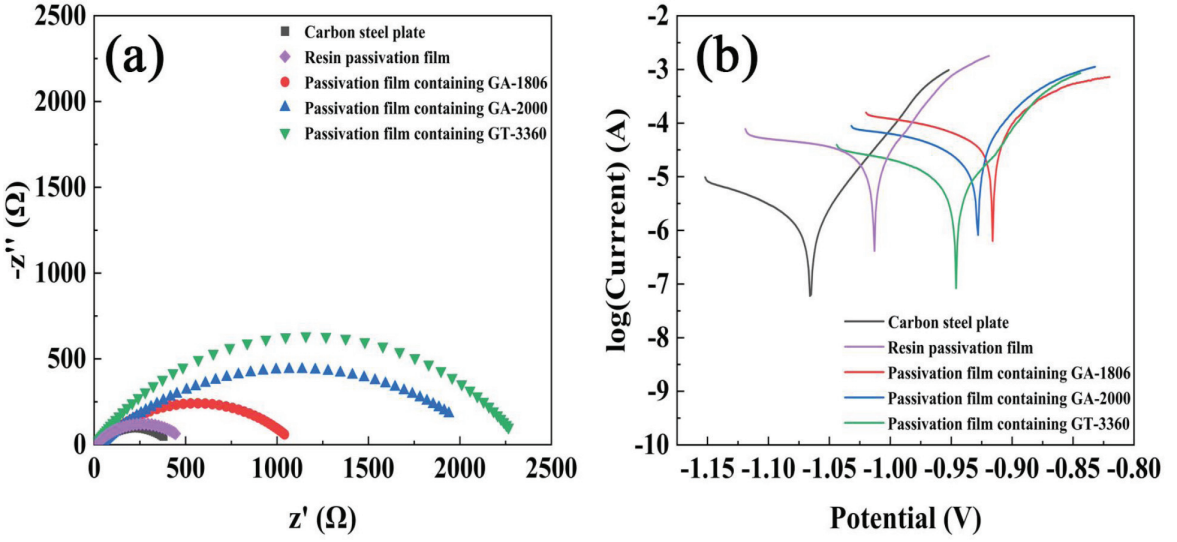

Figure 6: Electrochemical test results: a) EIS curves of samples coated with different composite passivation films; b) Tafel curves of samples coated with different composite passivation films

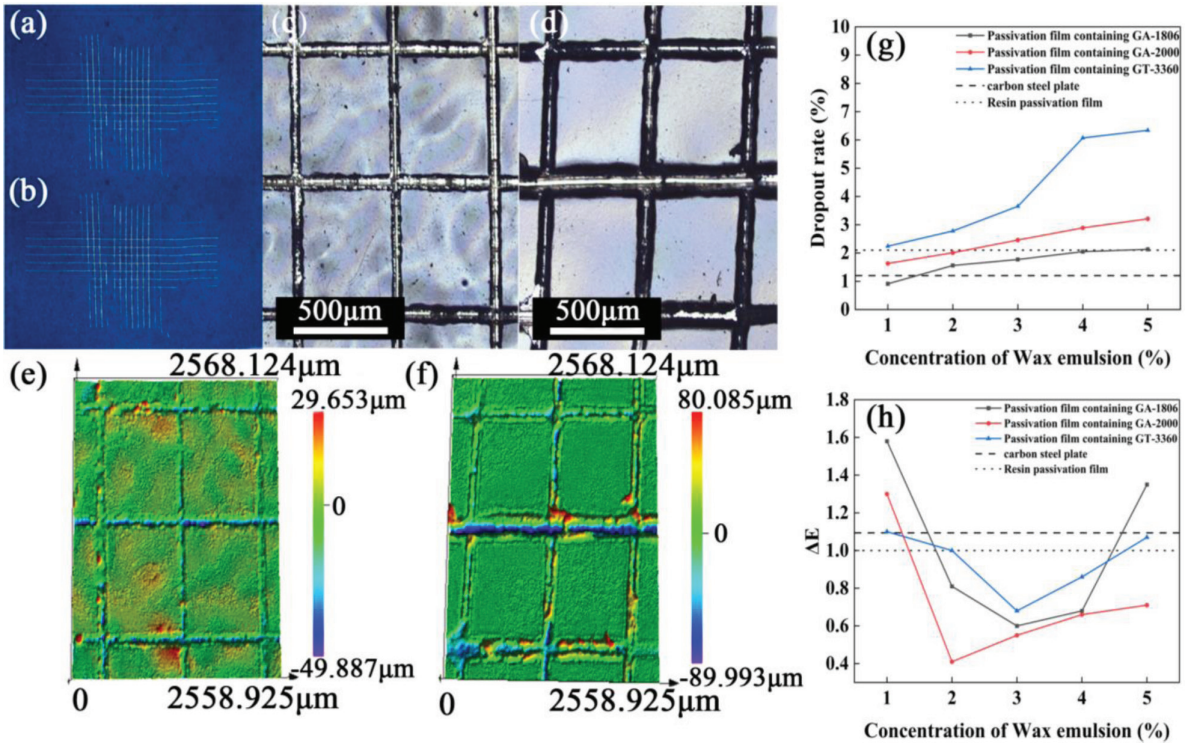

Figure 7: Results of the bonding force test: a) and b) are the optical photos of the coated resin passivation film and the coated composite passivation film with GA-2000 added samples for the paint resistance test; c) and d) are the low-magnification metallographic photos of the coated resin passivation film and the coated composite passivation film with GA-2000 added samples for the paint resistance test; e) and f) are the 3D surface topography images of the coated resin passivation film and the coated composite passivation film with GA-2000 added samples for the paint resistance test; g) is the paint resistance test result graph; h) is the fingerprint resistance test result graph.

tent with neutral salt spray test outcomes, further supporting the efficacy of wax emulsion in enhancing the passivation film's corrosion resistance.

3.4 Effect of wax emulsion on the adhesion of passivation film

A paintability resistance test was conducted on the passivation film, followed by observation of its surface and 3D surface morphologies. **Figure 7** illustrates the results. Passivation films containing GA-2000 and GA-1806 type wax emulsions demonstrated effective paintability resistance, as shown in **Figure 7g**, with no significant paint surface peeling observed after cross-cut testing. Metallographic images and 3D surface morphology analysis revealed uniform topcoat application and intact cross-cut sections. Conversely, passivation films incorporating GT-3360 exhibited poor paintability, with

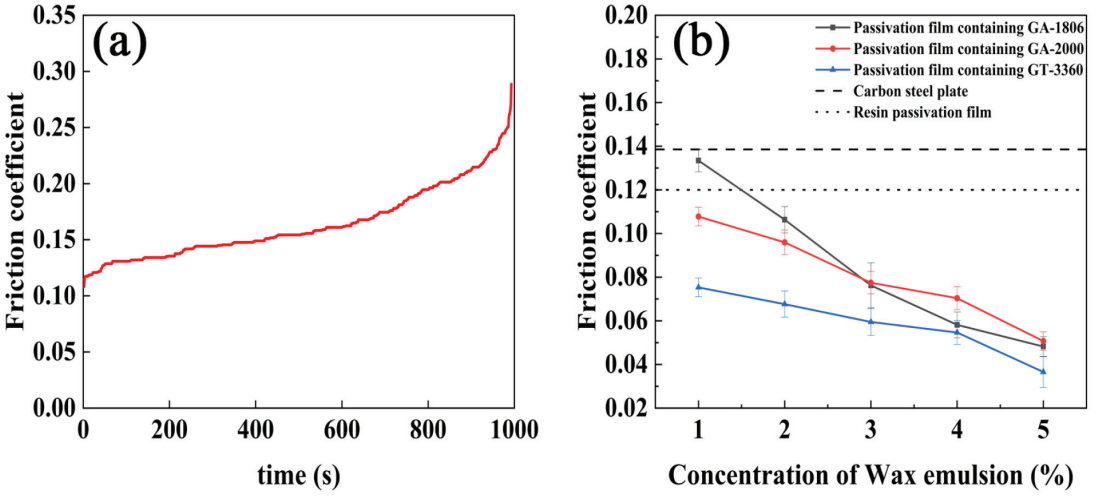

Figure 8: Influence of wax emulsion on the friction performance of the passivation film: a) The full friction test results for the samples coated with resin passivation film; b) The friction resistance test results after coating the samples with different wax-emulsion passivation films.

Table 2: Results of parallel friction resistance tests

Concentration of Wax Emulsion	Average Friction coefficient/1806	σ	Average Friction coefficient/2000	σ	Average Friction coefficient/3360	σ
1 %	0.13341	0.00512	0.10775	0.00425	0.07533	0.00427
2 %	0.10632	0.00602	0.09596	0.00561	0.06763	0.00599
3 %	0.07626	0.01031	0.07747	0.00513	0.05948	0.00616
4 %	0.05813	0.00587	0.07037	0.00528	0.05461	0.00546
5 %	0.04824	0.00449	0.05069	0.00427	0.03654	0.00705

performance deteriorating as wax emulsion concentration increased. Notably, at concentrations exceeding 2 %, extensive peeling of the topcoat occurred during cross-cut testing, attributed to the presence of paraffin particles in wax emulsions with smaller particle sizes, as depicted in Figure 1a. These paraffin particles, located at the passivation film-topcoat interface, reduce the surface energy of the passivation film due to their hydrophobic nature. Consequently, the bonding force between the passivation film and the topcoat diminishes, thereby compromising the passivation film's paintability.

The fingerprint resistance of the passivation film was evaluated, and the results are presented in Figure 7h. The data indicate that the addition of a wax emulsion initially reduces and then enhances the film's overall fingerprint resistance. Extreme particle sizes, either too large or too small, intensify fingerprint adhesion. The medium-sized GA-2000 achieves an optimal balance characterized by a distribution that is dense but non-overloaded.

3.5 Effect of wax emulsion on the friction resistance of the passivation film

Friction resistance tests were performed on passivation film-coated samples, with results depicted in **Figure 8**. In **Figure 8a**, the absence of wax emulsion is evident: the friction coefficient increased gradually over time, with a notable shift at 900 s. This abrupt change likely signifies complete wear-off of the passivation film, leading to friction between the ring block and the metal substrate and consequently a sharp rise in the friction coefficient. Before 900 s of friction, the experimental data suggest that friction primarily occurred between the ring block and the passivation film. During this period, the friction coefficient curve remained relatively stable, showing only marginal increments.

The experiments involved testing wax emulsions with varying particle sizes and concentrations. The average friction coefficient within the initial 600 s was designated as the passivation film's friction coefficient, as depicted in **Figure 8b**. The findings reveal that upon the addition of wax emulsion, the friction coefficients of all passivation films were lower than those of the control group. Moreover, a pattern emerged in which the friction coefficient decreased as the concentration of the wax emulsion increased. This occurrence can be attributed to paraffin's inherent lubricating properties. When formulated into an emulsion, paraffin's fluidity is enhanced. Within the passivation film, there is a degree of self-healing. During friction, the passivation film's thickness in the frictional region diminishes, prompting the supplementation of paraffin particles from the surrounding areas to enhance friction resistance. Notably, a reduction in the friction coefficient was observed with decreasing wax emulsion particle size at equivalent concentrations. This trend is likely due to the denser distribution of smaller paraffin particles on the passivation film's surface, as illustrated in **Figure 1a**. Consequently, a greater number of paraffin particles from the surrounding regions are incorporated into the frictional area during friction, leading to a decrease in the friction coefficient and an enhancement in the passivation film's friction resistance.

Each group of samples underwent three parallel experiments, and the standard deviation was computed using the following formula. The outcomes are detailed in **Table 2**. The calculations reveal a minor deviation in the friction coefficient from the mean, indicating stable results. The standard deviations (σ) hover around 0.5 %, affirming the substantial enhancement of friction resistance in the passivation film by the wax emulsion.

$$\sigma = \sqrt{\frac{\sum_{i=1}^{>N} (x_i - \mu)^2}{N}} \tag{1}$$

4 CONCLUSIONS

In this investigation, three distinct wax emulsions, namely GA-1806, GA-2000, and GT-3360, were utilized in the formulation of a composite passivation film alongside water-based polyurethane resin and surfactant. Through a comprehensive assessment encompassing structural analysis, surface morphology, corrosion resistance, frictional properties, and adhesion characteristics of the passivation film, GA-2000 demonstrated optimal performance at a 2 % dosage. This inclusion level yielded favorable outcomes, including reduced surface roughness, enhanced gloss, exceptional salt-spray resistance, and a lower friction coefficient, while maintaining excellent topcoat adhesion. Conversely, although GT-3360 exhibited notable hydrophobic and frictional attributes, its adverse influence on interfacial adhesion curtailed its practical viability. Consequently, the 2 % addition of GA-2000 wax emulsion was identified as the most advantageous dosage. At this concentration, the composite passivation film showcased elevated surface

gloss, diminished roughness, and enhanced frictional resilience. By prioritizing adhesion integrity, enhancements in self-repair capabilities and corrosion resistance were achieved, thereby substantially amplifying the overall performance of the system.

Acknowledgment

This work was supported by the Science and Technology Major Project of Gansu, China (Grant No. 22ZD6GB019)

5 REFERENCES

[1] Bijimi D, Gabe D R. Passivation studies using group VIA anions III anodic treatment of zinc. British Corrosion Journal, 18, no. 3 (**1983**), 138–41. doi:10.1179/000705983798273741

[2] Wilcox G D. Replacing chromates for the passivation of zinc surfaces. Transactions of the IMF, 81, no. 1 (**2003**), B13–15. doi:10.1080/00202967.2003.11871474

[3] Bastidas D M. Corrosion and protection of metals. Metals, 10, no. 4 (**2020**), 458. doi:10.3390/met10040458

[4] Pyun S I. Strategies of metal corrosion protection. Chemtexts, 7, no. 1 (**2021**), 2. doi:10.1007/s40828-020-00121-y

[5] Berger R, Bexell U, Mikael Grehk T, Hörnström S E. A comparative study of the corrosion protective properties of chromium and chromium free passivation methods. Surface and Coatings Technology, 202, no. 2 (**2007**), 391–97. doi:10.1016/j.surfcoat.2007.06.001

[6] Haiyang F, Bo G, Yingwei Z, Pengfei X. Effects of silanes on the structure and properties of chromium-free passivation. Science of Advanced Materials, 12, no. 7 (**2020**), 1012–18. doi:10.1166/sam.2020.3750

[7] Prakash B S, Balaraju J N. Chromate (Cr^{6+})-free surface treatments for active corrosion protection of aluminum alloys: a review. Journal of Coatings Technology and Research, 21, no. 1 (**2023**), 105–35. doi:10.1007/s11998-023-00831-1

[8] Peltier F, Thierry D. Review of Cr-free coatings for the corrosion protection of aluminum aerospace alloys. Coatings, 12, no. 4 (**2022**), 518. doi:10.3390/coatings12040518

[9] Vaghefinazari B, Wierzbicka E, Visser P, Posner R, Arrabal R, Matykina E, Mohedano M, Blawert C, Zheludkevich M, Lamaka S. Chromate-free corrosion protection strategies for magnesium alloys-a review: PART I-pre-treatment and conversion coating. Materials, 15, no. 23 (**2022**), 8676. doi:10.3390/ma15238676

[10] Yong Q, Liao B, Huang J, Guo Y, Liang C, Pang H. Preparation and characterization of a novel low gloss waterborne polyurethane resin. Surface and Coatings Technology, 341 (**2018**), 78–85. doi:10.1016/j.surfcoat.2018.01.012

[11] Król P, Król B, Stagraczyński R, Skrzypiec K. Waterborne cationomer polyurethane coatings with improved hydrophobic properties. Journal of Applied Polymer Science, 127, no. 4 (**2013**), 2508–19. doi:10.1002/app.37552

[12] Ferguson J, Petrovic Z. Thermal stability of segmented polyurethanes. European Polymer Journal, 12, no. 3 (**1976**), 177–81. doi:10.1016/0014-3057(76)90050-1

[13] Valadez T N, Norton J R, Neary M C. The reaction of cp*(Cl)M(diene) (M = Ti, Hf) with isonitriles. Journal of the American Chemical Society, 137, no. 32 (**2015**), 10152-5. doi:10.1021/jacs.5b06654

[14] Chen G nan, Chen K nan. Dual-curing of anionic aqueous-based polyurethanes at ambient temperature. Journal of Applied Polymer Science, 67, no. 9 (**1998**), 1661–71. doi:10.1002/(SICI)1097-4628(19980228)67:9<1661::AID-APP18>3.0.CO;2-X

[15] Yang S, Xiao H X, Higley D P, Kresta J, Frisch K C, Farnham W B, Hung M H. Novel fluorine-containing anionic aqueous polyurethanes. Journal of Macromolecular Science, Part a 30, nos. 2–3 (**1993**), 241–52. doi:10.1080/10601329308009402

[16] Wang H H, Lin Y T. Silicon-containing anionic water-borne polyurethane with covalently bonded reactive dye. Journal of Applied Polymer Science, 90, no. 8 (**2003**), 2045–52. doi:10.1002/app.12797

[17] Li Y, Noordover B A J, Van Benthem R A T M, Koning C E. Chain extension of dimer fatty acid- and sugar-based polyurethanes in aqueous dispersions. European Polymer Journal, 52 (**2014**), 12–22. doi:10.1016/j.eurpolymj.2013.12.007

[18] Li X, Wang W, Wu Y, Kang H, Guo E, Li J, Chen Z, Xu Y, Wang T. Improving the corrosion resistance of 7055 alloy by manipulating passivation film through trace addition of TiB_2 nanoparticles. Applied Surface Science, 656 (**2024**), 159722. doi:10.1016/j.apsusc.2024.159722

[19] Yu M, Feng J, Yang Q, Dang Z, Zhang L. Inhibition of organosilane/ATP@HQ self-healing passivator for pyrite oxidation. Chemosphere, 287 (**2022**), 132342. doi:10.1016/j.chemosphere.2021.132342

[20] Wang Z, Feng K, Li Z, Lu F, Huang J, Wu Y, Chu P K. Self-passivating carbon film as bipolar plate protective coating in polymer electrolyte membrane fuel cell. International Journal of Hydrogen Energy, 41, no. 13 (**2016**), 5783–92. doi:10.1016/j.ijhydene.2016.02.076

[21] Wang G, Zhou Z, Zhang K, Wu L, Shi X, Zhang X. Study on corrosion resistance of passive film promoted by natural rosin-based passive sealant. Journal of Materials Research and Technology, 28 (**2024**), 1679–93. doi:10.1016/j.jmrt.2023.12.097

[22] Petrunin M A, Gladkikh N A, Maleeva M A, Rybkina A A, Terekhova E V, Yurasova T A, Ignatenko V E, Maksaeva L B, Kotenev V A, Tsivadze A Yu. Improving the anticorrosion characteristics of polymer coatings in the case of their modification with compositions based on organosilanes. Protection of Metals and Physical Chemistry of Surfaces, 57, no. 2 (**2021**), 374–88. doi:10.1134/S2070205121020076

[23] Ciesińska W, Liszyńska B, Zieliński J. Selected thermal properties of polyethylene waxes. Journal of Thermal Analysis and Calorimetry, 125, no. 3 (**2016**), 1439–43. doi:10.1007/s10973-016-5706-1

[24] Bayer I S, Fragouli D, Martorana P J, Martiradonna L, Cingolani R, Athanassiou A. Solvent resistant superhydrophobic films from self-emulsifying carnauba wax–alcohol emulsions. Soft Matter, 7, no. 18 (**2011**), 7939–43. doi:10.1039/C1SM05710C

[25] Wang W, Zhu Y, Cao J, Guo X. Thermal modification of southern pine combined with wax emulsion preimpregnation: effect on hydrophobicity and dimensional stability. Holzforschung, 69, no. 4 (**2014**), 405–13. doi:10.1515/hf-2014-0106

[26] Zhang J, Tian D, Lin M, Yang Z, Dong Z. Effect of resins, waxes and asphaltenes on water-oil interfacial properties and emulsion stability. Colloids and Surfaces, A: Physicochemical and Engineering Aspects, 507 (**2016**), 1–6. doi:10.1016/j.colsurfa.2016.07.081

[27] Hou B, Chen W, Cao Z. A process for the preparation of emulsified wax. Petroleum Science and Technology, 25, no. 12 (**2007**), 1549–55. doi:10.1080/10916460600695389

[28] Fang D, He F, Xie J, Xue L. Calibration of binding energy positions with C1s for XPS results. Journal of Wuhan University of Technology-Mater. Sci. Ed., 35, no. 4 (**2020**), 711–18. doi:10.1007/s11595-020-2312-7

[29] Frankcombe T J, Liu Y. Interpretation of oxygen 1s X-ray photoelectron spectroscopy of ZnO. Chemistry of Materials, 35, no. 14 (**2023**), 5468–74. doi:10.1021/acs.chemmater.3c00801

[30] Olayo M G, Alvarado E J, González-Torres M, Gómez L M, Cruz G J. Quantifying amines in polymers by XPS. Polymer Bulletin, 81, no. 3 (**2023**), 2319–28. doi:10.1007/s00289-023-04829-y

[31] Koshizaki N, Umehara H, Oyama T. XPS characterization and optical properties of Si/SiO_2, Si/Al_2O_3 and Si/MgO co-sputtered films. Thin Solid Films, 325, no. 1 (**1998**), 130–36. doi:10.1016/S0040-6090(98)00512-4

[32] Long Y, Liu C, Peng S. Enhanced performance of a green inorganic-based passive film on the batch hot-dip galvanized steel by organic additives. International Journal of Electrochemical Science, 15, no. 3 (**2020**), 2568–80. doi:10.20964/2020.03.44

[33] Chen C, Chen J, Zhang S, Cao J, Wang W. Forming textured hydrophobic surface coatings via mixed wax emulsion impregnation and drying of poplar wood. Wood Science and Technology, 54, no. 2 (**2020**), 421–39. doi:10.1007/s00226-020-01156-7

[34] Chen Y, Chen Q, Ding J, Liu Q, Yuan S, Yu H, Guo Y, Cheng Y, Qian H, Yao W. Glutenin phase transition as a method of fabricating primer for superhydrophobic and corrosion-resistant coating. Journal of Colloid and Interface Science, 681 (**2025**), 169–81. doi:10.1016/j.jcis.2024.11.152

[35] Lv Y, Sun Y, Deng C, Fan X, Li S, Wang C, Yang Y, Zhang Y, He C. Preparation, corrosion and tribological properties evolution of self-lubricating Al_2O_3-TiO_2 coatings with superior anti-corrosion. Surface and Coatings Technology, 498 (**2025**), 131849. doi:10.1016/j.surfcoat.2025.131849

[36] Zhou S, Jia X, Tian R, Song H. Self-lubricating, self-healing and anti-corrosion coating with ultra-short run-in period. Tribology International, 196 (**2024**), 109706. doi:10.1016/j.triboint.2024.109706